

Joseph A. Grim¹, Robert M. Rauber
University of Illinois at Urbana-Champaign, Urbana, IL

1. INTRODUCTION

Mesoscale convective systems (MCSs) are common during the late spring and summer across the central United States (Johns 1993) and are often associated with strong straight-line winds. MCS squall lines or squall line segments sometimes form a bow-shaped line of convective cells (termed a bow echo) that can be associated with swaths of damaging straight-line winds (e.g., Nolen 1959). From pioneering studies of Fujita (see review by Weisman 2001) and subsequent numerical studies (e.g., Weisman 1993), it is known that the strong straight-line surface winds associated with bow echoes can originate within downdrafts generated along and behind convective lines. Studies have also shown that the strong straight-line surface winds are often associated with the presence and descent of the RIJ to the surface (e.g., Duke and Rogash 1992; Miller and Johns 2000).

Observational and numerical studies show that the RIJ develops in tandem with the formation of one or possibly two mid-level low pressure centers, one generated by a hydrostatically-induced negative pressure perturbation immediately under the upshear-tilted warm convective updrafts (e.g., Smull and Houze 1987; Weisman and Davis 1998) and another, near the back edge of the stratiform region, the result of combined effects of latent heat release in the mesoscale updraft and evaporative cooling enhanced by melting in the mesoscale downdraft (e.g., Smull and Houze 1987).

Between 1900 UTC 26 August and 0430 UTC 27 August 2003, a widespread swath of damaging winds occurred across the Midwestern United States. Damaging winds were first reported along the Indiana-Michigan border, with subsequent reports along a swath extending east-southeastward through northern Ohio and into western Pennsylvania, northern West Virginia, and far western Maryland. A total of 87 counties reported damaging winds. The exceptionally widespread damage from straight-line winds, and the nature of the damage qualified this

event as a derecho (Johns and Hirt 1987). This MCS displayed an unusual feature that has not been documented in previous literature: dual RIJs at different altitudes that appeared to merge behind the leading convective line at locations concurrent with the most concentrated surface damage. The purpose of this note is to document this feature and consider possible reasons for its occurrence.

2. DUAL REAR INFLOW JET STRUCTURE

The initial convection that developed into the MCS initiated over north-central Illinois at 1600 UTC 26 August (not shown). The system quickly developed into a generally northeast-southwest oriented, bow-shaped line of convection as it propagated east-southeastward across northern Illinois to north-central Indiana. By 2100 UTC, a widespread stratiform rain region had developed to the rear of the convective line (not shown), along with storm-relative rear-to-front flow at mid-levels and front-to-rear flow aloft.

Surface wind damage was reported with this system beginning around 1900 UTC (Fig. 1). By 2100 UTC eight severe thunderstorm warnings were in effect with this derecho. The leading convective line, with peak base scan reflectivities of 53 dBZ from the Northern Indiana (KIWX) radar, extended from 40 km east of the Indiana-Michigan-Ohio border to just northeast of Huntington, Indiana (Fig. 2a). A 100 km wide trailing stratiform region was present to the rear of the system. Outbound radial velocities as high as 37 m s⁻¹ were observed from the base velocity scan at 1000 m (all heights relative to the elevation of the KIWX radar) just to the rear of the leading convective line (Fig. 2b). Mesovortices were present on the fringes of the system and may have been associated with damaging surface winds in those areas.

The magnitude of "rear inflow" depends upon the reference frame used for system motion. A variety of reference frames have been used in previous studies to determine system motion. These reference frames include: the trailing precipitation boundary (e.g., Smull and Houze 1987), the leading convective line (e.g., Kessinger et al. (1987), the cells along the leading convective line (e.g., Klimowski 1994), the most stationary frame of reference (e.g., Jorgensen et al. 1997) and from winds measured from nearby soundings (e.g., Knupp et al. 1998).

¹Corresponding author address: Joseph A. Grim, Dept. of Atmospheric Sciences, Univ. of Illinois, Urbana, IL 61801; e-mail: jgrim@uiuc.edu.

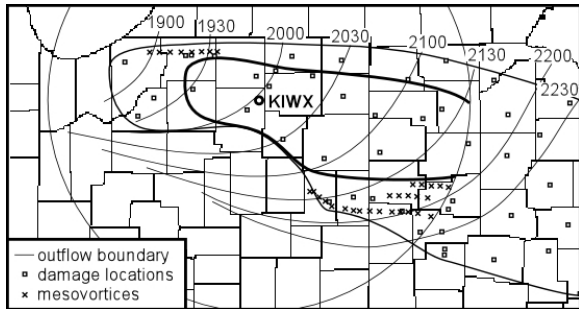


Figure 1. Map of surface wind damage with individual reports indicated by small squares. The thick line encompasses the region in which the dual RIJ structure was present near the rear of the convective line. The moderately thick line encompasses the region where surface wind damage was reported. The thin circle is the max. range for radial velocity values from the KIWX WSR-88D radar. Thin lines are isochrones of the location of the outflow boundary associated with the MCS. Locations of mesovortices from each radar sweep indicated by the “x”s.

In the analyses that follow, we show the ground-relative radial velocity from the KIWX radar. Estimates of the magnitude of the rear inflow were made by considering the projection of the radial velocity in the direction of the system motion vector using two frames of reference. The first reference frame used the motion of the rear edge of the trailing stratiform precipitation (17 m s^{-1} at 117°), and the second, the average forward motion of the cells along the leading convective line (26 m s^{-1} at 108°).

Figures 2 and 3 show the horizontal and vertical structure of the MCS at three times during which the dual RIJ structure was best observed by the KIWX radar. The cross-sections in Fig. 3 were chosen to elucidate the structure of the RIJ and the parent MCS. When examining these figures, it is important to note that the radial velocities are relative to the radar and not to the cross-section. The percentage of the cross-section parallel wind component observed within the radial velocity field is listed across the top of each panel in Figs. 3b, e, and h. The geometry is important to the interpretation of the structure of the RIJ, as well as other flows within the system, since the percentage of the cross-section parallel wind captured by the radial velocity measurements is strongly dependent on the angle between the radar beam and the cross-section.

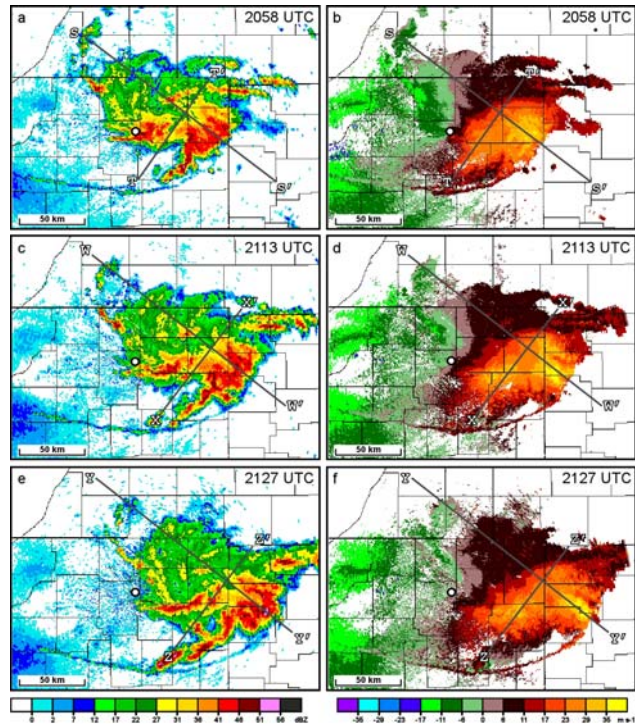


Figure 2. Base scan radar reflectivity (a, c, and e) and ground-relative radial velocity (b, d, and f) from the KIWX WSR-88D radar (indicated by a small circle) at (a and b) 2058 UTC, (c and d) 2113 UTC, and (e and f) 2127 UTC 26 August 2003. Lines denote cross-sections displayed in Fig. 4 (a)-(f).

Cross-sections across the system at the three times corresponding to Figs. 2a, c, and e revealed that the leading convective line was nearly vertical (Figs. 3a, d, and g.) A radar bright band was evident just below 4000 m within the trailing stratiform region at each time. The primary storm updraft was indicated at the leading convective line by a minimum in the radial velocity field. The flow was seen to be divergent at the top of this updraft. Anvils extended forward and rearward $\sim 50 \text{ km}$ from the forward and rear edges of the surface precipitation.

Two branches of the RIJ are evident in the radial velocity cross-sections (Fig. 3b, e and h). The flow in each branch of the RIJ is indicated by following the axes of maximum inbound velocities on the left side of the cross-section (to the left of the 0% position) and maximum outbound velocities on the right side of the cross-section. The upper branch of the RIJ appears as a maximum of inbound velocities at $\sim 9000 \text{ m}$ on the left side of the cross-section. This branch descended to $\sim 5000 \text{ m}$ 15 km behind the leading convective line, as evident in the local maxima

in outbound ground-relative radial velocities. The lower branch of the RIJ appears as a maximum of inbound velocities at ~5500 m at the left edge of the trailing stratiform region. This branch descended to ~1500 m about 50 km behind the leading convective line. A maximum outbound radial velocity of 41 m s⁻¹ was observed just to the rear of the convective line at 2127 UTC (Fig. 2f). The actual (ground-relative) magnitude of the RIJ was potentially as large as 48 m s⁻¹. Surface wind speeds at this time and location were reported as high as 36 m s⁻¹, implying that the lower branch of the RIJ descended to the surface.

Based on the projection of the radial velocity into the cross-sectional plane shown on Fig. 2b, the lower branch of the RIJ shown in Figs. 3b and 3e crossed the trailing edge of the precipitation at a relative speed of 4 m s⁻¹ and 3 m s⁻¹, respectively, while at the last time (Fig. 3h) the flow had diminished sufficiently, so that there was no longer rear-to-front flow across the rear edge. At each time, the rear inflow in the lower branch accelerated toward the leading convective line. Just behind the convective line, the line-relative rear inflow, based on the projection of the radial velocities in Figs. 3b, 3e and 3h was 32 m s⁻¹, 18 m s⁻¹ and 18 m s⁻¹, respectively.

Based on the shape of the zero velocity isodop in Fig. 3b, the flow at the altitude of the upper branch of the RIJ was at an angle of 17° (counter-clockwise) with respect to the lower branch. Taking into account this angle and the projection of the radial velocities into the cross-sections in Figs. 3b and e, the speed of the upper branch of the rear inflow across the trailing precipitation boundary was 5 m s⁻¹. By the last time (Fig. 3h), the flow at the back edge of the system had weakened sufficiently so that it could no longer be considered rear inflow. The upper branch of the RIJ slowly accelerated toward the front of the system, reaching a line-relative speed of 3 - 8 m s⁻¹ at an altitude of ~ 4 km.

Figures 3c, f, and i show the ground-relative radial velocity along cross-sections parallel to the leading convective line (perpendicular to the direction of the rear inflow.) These cross-sections reveal that the dual RIJ structure was present over a broad area within the MCS. Two (~50 km wide) maxima in outbound radial velocity, marked by heavy dashed lines, are evident at different elevations in each panel.

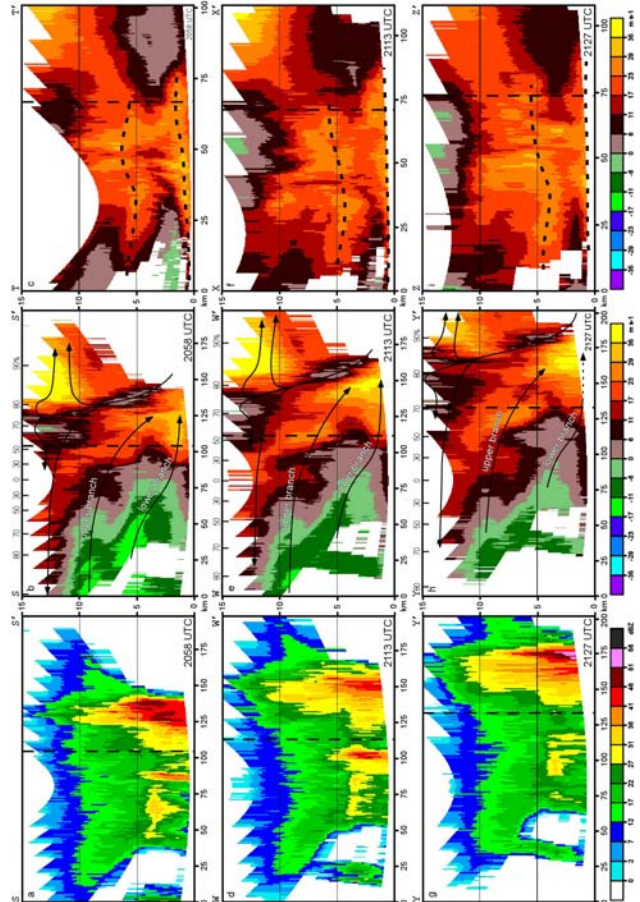


Figure 3. Radar cross-sections of reflectivity (a), (d) and (g) and ground-relative radial velocity (b), (c), (e), (f), (h), and (i) for cross-sections denoted on Fig. 3. Arrows on (b), (e) and (h) show system-relative flow. The percentage of the cross-section parallel wind component observed within the radial velocity field is listed across the top of panels (b), (e), and (h). Heavy dashed lines denote intersections of the two cross-sections.

The most significant straight-line wind damage was reported during the period in which the dual-RIJ structure was present (1930-2145 UTC). Surface straight-line winds as high as 36 m s⁻¹ were reported and resulted in downed trees and power lines, as well as damage to farm buildings (Storm Prediction Center 2003). Based on these damaging wind reports, the lower branch of the RIJ shown in Fig. 3 must have descended to the surface. The upper branch of the RIJ may also have descended and merged with the lower branch, contributing to the severe winds, although it is difficult to infer this directly from the radial velocities shown in the cross-sections.

It was not possible to obtain analyses of pressure aloft, so we can only speculate on possible mechanisms for the presence of the dual RIJs. In the studies by Smull and Houze (1987) and Klimowski (1994), a single RIJ was forced by separate mid-level low pressure centers, resulting in separate maxima within the same RIJ. It may be possible that the dual RIJs in this case were produced by two separate mid-level low-pressure centers. One possibility could be that the upper branch developed as a result of a negative pressure perturbation associated with the upshear-tilted updraft, while the lower branch may have been associated with diabatic processes near the back edge of the stratiform region. Additional studies are necessary to determine if these mechanisms would indeed be capable of producing a dual RIJ structure.

3. SUMMARY

The unique features of this MCS were the dual RIJs. The upper branch descended gradually from ~9000 m at the rear of the system to ~5000 m about 15 km behind the leading convective line, while the lower branch descended from ~5500 m at the rear of the system to ~1500 m about 50 km behind the leading convective line, reaching the surface at the convective line. The most spatially continuous and extensive damage from this system occurred while both branches of the RIJ were present. It is unknown how often this feature may occur in other MCSs. The ongoing analysis of the extensive data set from the Bow Echo and MCV EXperiment (BAMEX; Davis et al. 2004) may provide further insight into processes that can lead to this unusual structure.

ACKNOWLEDGEMENTS

This research was supported by the National Science Foundation under grant NSF-ATM-0413824.

REFERENCES

Davis, C., N. Atkins, D. Bartels, L. Bosart, M. Coniglio, G. Bryan, W. Cotton, D. Dowell, B. Jewett, R. Johns, D. Jorgensen, J. Knievel, K. Knupp, W.-C. Lee, G. McFarquhar, J. Moore, R. Przybylinski, R. Rauber, B. Smull, R. Trapp, S. Trier, R. Wakimoto, M. Weisman,

C. Ziegler, 2004: The bow echo and MCV experiment. *Bull. Amer. Meteor. Soc.*, **85**, 1075-1093.
Duke, J. W., and J. A. Rogash, 1992: Multiscale review of the development and early evolution of the 9 April 1991 derecho. *Wea. Forecasting*, **7**, 623-635.
Johns, R. H., 1993: Meteorological conditions associated with bow echo development in convective storms. *Wea. Forecasting*, **8**, 294-300.
—, and W. O. Hirt, 1987: Derechos: Widespread convectively induced windstorms. *Wea. Forecasting*, **2**, 32-49.
Jorgensen, D. P., M. A. LeMone, and S. B. Trier, 1997: Structure and evolution of the 22 February 1993 TOGA COARE squall line: Aircraft observations of precipitation, circulation, and surface energy fluxes. *J. Atmos. Sci.*, **54**, 1961-1985.
Kessinger, C. J., P. S. Ray, and C. E. Hane, 1987: The Oklahoma squall line of 19 May 1977. Part I: A multiple Doppler analysis of convective and stratiform structure. *J. Atmos. Sci.*, **44**, 2840-2864.
Klimowski, B. A., 1994: Initiation and development of rear inflow within the 28-29 June 1989 North Dakota mesoconvective system. *Mon. Wea. Rev.*, **122**, 765-779.
Knupp, K. R., B. Geerts, and S. J. Goodman, 1998: Analysis of a small vigorous mesoscale convective system in a low-shear environment. Part I: Formation, radar echo structure and lightning behavior. *Mon. Wea. Rev.*, **126**, 1812-1836.
Miller, D. J., and R. H. Johns, 2000: A detailed look at extreme wind damage in derecho events. Preprints, *20th Conf. on Severe Local Storms*, Orlando, FL, Amer. Meteor. Soc., 52-55.
Nolen, R. H., 1959: A radar pattern associated with tornadoes. *Bull. Amer. Meteor. Soc.*, **40**, 277-279.
Smull, B. F., and R. A. Houze, 1987: Rear inflow in squall lines with trailing stratiform precipitation. *Mon. Wea. Rev.*, **115**, 2869-2889.
Storm Prediction Center Storm Reports, 2003: http://www.spc.noaa.gov/climo/reports/030826_rpts.html
Weisman, M. L., 1993: The genesis of severe, long-lived bow echoes. *J. Atmos. Sci.*, **50**, 645-670.
—, and C. A. Davis, 1998: Mechanisms for the generation of mesoscale vortices within quasi-linear convective systems. *J. Atmos. Sci.*, **55**, 2603-2622.
—, 2001: Bow echoes: A tribute to T. T. Fujita. *Bull. Amer. Meteor. Soc.*, **82**, 97-116.